Light intensity dependence of a two-photon catalytic cycle: Photoionization via absorption–electron transfer–absorption

2 **AUTHORS**, INCLUDING:

Valentin E. Zubarev
Martin Luther University Halle-Wittenb…
98 PUBLICATIONS **395** CITATIONS

Light intensity dependence of a two-photon catalytic cycle: photoionization via absorption–electron transfer–absorption

Martin Goez [*], Valentin Zubarev

Fachbereich Chemie, Martin-Luther Universität, Halle–Wittenberg, Kurt–Mothes-Strasse 2, D-06120 Halle/Saale, Germany

Received 28 December 1999

Abstract

The kinetics of the title mechanism, in which the substrate is excited by a light pulse and the radical anion resulting from quenching by a suitable electron donor is then photoionized within the duration of the same pulse, is analyzed theoretically and experimentally. A characteristic of this mechanism as compared to other two-photon ionizations with an intervening chemical step is the regeneration of the substrate. As a consequence, the yield of hydrated electrons $e_{aq}^{•-}$ can grossly exceed the substrate concentration; for continuous illumination, it is only limited by depletion of the donor, which must be present in high excess anyway to ensure high quenching rates and efficiencies. When the absorption steps are much faster than the quenching, the amount of $e_{aq}^{•-}$ produced within a given time depends on the shape of the excitation pulse and saturates at high light intensities, whereas in the opposite case the yield of $e_{aq}^{•-}$ is independent of the pulse envelope and becomes a linear function of the integrated intensity I in the limit of high I. Tests of the theoretical predictions by laser flash photolysis (pulse duration, 20 ns) of 1,5-anthraquinonedisulfonate or 4-carboxybenzophenone with triethylamine as the quencher in water gave excellent agreement. Substantial quantum yields (0.16 and 0.23) were found for the photoionizations of the two radical anions at 308 nm. © 2000 Elsevier Science B.V. All rights reserved.

1. Introduction

Photoionization is an important process with respect to light-induced damage in biological materials [1,2]. It is well established that it can occur monophotonically, biphotonically, or by successive absorption of two photons with the involvement of an intermediate [3]. In most cases where the latter pathway is realized, this intermediate is an electronically excited state of the substrate.

Two-photon ionizations with intervening chemical step (Scheme 1) are comparatively rare, most examples being confined to ionization of a radical generated by a photoinduced homolytic reaction [4–6]. [1] Yet, when photoionizations are to be used to generate hydrated electrons $e_{aq}^{•-}$ by laser flash photolysis, which is both much more selective and much less costly than by pulse radiolysis, a kinetic advantage of such a type of two-photon ionization might be that the lifetime of radicals is often longer than that of excited states because only bimolecular deactivation routes are open to the former. We have recently found [10,11] a variant that appears tailored to this purpose, namely an absorption–electron transfer–absorption

---

[1] Conceptually related two-photon processes are UV/VIS induced photoionizations of intermediates produced by pulse radiolysis [7–9].

[*] Corresponding author.

$$S \xrightarrow{h\nu} S^* \longrightarrow X \xrightarrow{h\nu} P + e^{\bullet-}_{aq}$$
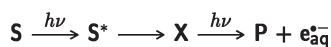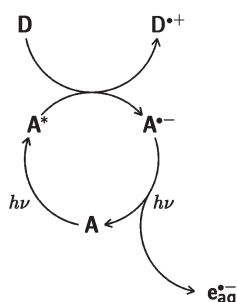
Scheme 1.

Scheme 2.

pathway to $e^{\bullet-}_{aq}$ (Scheme 2). The fundamental difference to the other known ionization routes via absorption–chemical reaction–absorption is that the substrate is regained in the photoionization step, so the whole sequence is a catalytic cycle with respect to the substrate, the sacrificial donor being ionized in effect. Another significant advantage is thermodynamical: the ionization of the radical anion is favored by the formation of a stable product (the substrate) as compared to photoionization of a radical [4–6], which must be accompanied by the formation of an unstable intermediate (a carbocation).

In this paper, we deal with the important case of both photoreactions occurring during the same laser flash. We theoretically and experimentally analyze the dependence of the electron yield on the intensity of the exciting light, which is the key factor when these mechanisms are to be used for efficient generation of $e^{\bullet-}_{aq}$ in a given reaction system.

2. Experimental section

The intensity dependent measurements were carried out with an excimer laser (Radiant Dyes RD-EXC-150; 308 nm; duration of the excitation pulse, $\approx$20 ns; maximum energy impinging on the measuring cell, about 36 mJ per pulse). The intensity was varied by using metal-grid filters. For the quenching experiments, a Nd:YAG laser (Continuum Surelite II-10; 355 nm; $\approx$5 ns; about 35 mJ) was used. The dimensions of the excited volume were 2 mm × 4 mm × 2 mm in the directions of the laser beam, the monitoring light, and perpendicular to the preceding two. To avoid a depletion of the reactants, repetition rates were kept below 0.3 Hz, and the solutions were allowed to flow through the cell. Except for a photomultiplier with increased sensitivity in the red (Hamamatsu R 928), detection was done in the standard way. The rise time of the detection system was 5 ns, which was essentially limited by the amplifier. Because of the well-defined geometrical arrangement, absolute concentrations of the transients can be reliably determined with this experimental setup.

All chemicals were obtained commercially in the highest purity available (>99.5%) and used as received. The quality of the solvent, ultrapure Millipor MilliQ water (resistance 18.2 MΩcm^{-1}), was tested in regular intervals by control experiments (photoionization at 308 nm of dilute solutions of the phenolate anion), in which the half-life of $e^{\bullet-}_{aq}$ was monitored. Before each measurement, oxygen was removed by bubbling inert gas through the solution; the all-glass flow system, which was driven by a slightly elevated pressure of inert gas, prevented oxygen uptake during the measuring time. The pH value was adjusted with NaOH.

3. Results and discussion

3.1. Formal kinetics

For sufficiently small optical path lengths, which is realized in our experiments, the two light-induced steps in Scheme 2 are first order in the substrate **A** and the radical anion **A**$^{\bullet-}$, respectively, with rate constants that are (possibly complicated) functions of time because the envelope of the laser pulse is not rectangular. However, the *ratio* of the two rate constants does not depend on time; it is determined by the extinction coefficients of **A** and **A**$^{\bullet-}$ and by the quantum yields of formation of the excited state **A*** that undergoes electron-transfer

quenching [2] and of photoionization of the radical anion, ϕ_1 and ϕ_2. Hence, we write the first rate "constant" as $k_1 f(t)$ and the second as $k_2 f(t)$, where $f(t)$ is the effective envelope (in energy per time) of the laser pulse, and k_1 and k_2 are constant proportionality factors with the dimension of a reciprocal energy. Radiationless decay (rate constant k_d) of A^* competes with quenching by the donor D (with a pseudo-first-order rate constant k_q that contains the donor concentration).

Depletion of the substrate during the laser pulse must be taken into account. By using the mass balance to eliminate the differential equation for this species and expressing the concentrations of A^* and $A^{\bullet-}$ relative to its starting concentration a_0, one arrives at

$$\frac{d}{dt}[A^*]/a_0 = k_1 f(t) - \left\{ k_1 f(t) + k_q + k_d \right\}[A^*]/a_0 - k_1 f(t)[A^{\bullet-}]/a_0, \tag{1}$$

$$\frac{d}{dt}[A^{\bullet-}]/a_0 = k_q[A^*]/a_0 - k_2 f(t)[A^{\bullet-}]/a_0. \tag{2}$$

The concentration of the electron can be found by integrating $k_2 f(t)[A^{\bullet-}]$ over the duration of the laser pulse. At the end of the pulse, some amount of A^* is present, and subsequently a fraction $k_q/(k_d + k_q)$ of this is converted into $A^{\bullet-}$. The expressions given below for $[A^{\bullet-}]$ include this correction.

General solutions for arbitrary pulse shapes $f(t)$ must be obtained numerically. For the simplest case, a rectangular pulse, a closed-form solution is given in Appendix A.

Two limiting cases can be distinguished. When the light-induced steps are much faster than the quenching, the measured concentration of $A^{\bullet-}$ approaches that of A^* at the end of the pulse times the Stern–Volmer factor $k_q/(k_d + k_q)$, and that of $e_{aq}^{\bullet-}$ is limited by the quenching process. Hence, for

a fixed duration of the laser pulse, both $[A^{\bullet-}]$ and $[e_{aq}^{\bullet-}]$ exhibit saturation behavior when the light intensity is increased (compare the analytical result in Appendix A). Typical concentration traces are shown at the top of Fig. 1. As can be seen, the envelope of the laser pulse has a noticeable influence on the curves, especially on that of $[e_{aq}^{\bullet-}]$, in this limit.

When, on the other hand, quenching is much faster than is the formation of A^*, one may lump together excitation [2] and quenching as a single step characterized by the rate constant $k_1 f(t)$. The concentration of A^* approaches zero in this case. With the mass balance, Eqs. (1) and (2) thus reduce to a single differential equation:

$$\frac{d}{dt}[A^{\bullet-}]/a_0 = f(t)\{k_1 - (k_1 + k_2)[A^{\bullet-}]/a_0\}. \tag{3}$$

The solution of Eq. (3),

$$[A^{\bullet-}]/a_0 = \frac{k_1}{k_1 + k_2}\left\{ 1 - \exp\left[-(k_1 + k_2)\int_0^t f(t')\,dt' \right] \right\}$$

$$= \frac{k_1}{k_1 + k_2}\{1 - \exp[-(k_1 + k_2)I]\}, \tag{4}$$

is seen to depend no longer on the shape of the laser pulse but only on the integrated total light intensity I. The same holds for the formation of $e_{aq}^{\bullet-}$, where integration of $k_2 f(t)[A^{\bullet-}]$ yields

$$[e_{aq}^{\bullet-}]/a_0 = \frac{k_1 k_2}{(k_1 + k_2)^2}\{-1 + (k_1 + k_2)I + \exp[-(k_1 + k_2)I]\}. \tag{5}$$

Neglecting the depletion of A would only lead to a replacement of the term $(k_1 + k_2)$ by k_2 everywhere in Eqs. (3)–(5) but would not change the general functional forms. In this limit of fast quenching, only $[A^{\bullet-}]$ goes into saturation when the light intensity is increased but $[e_{aq}^{\bullet-}]$ increases linearly. A typical example is displayed at the bottom of Fig. 1. Owing to the unimportance of the pulse envelope under these circumstances, the only parameters needed to correct the experimental data for inner filter effects (see Section 3.2) are the extinction coefficients of all species at the excitation wavelength.

---

[2] With our substrates (ketones or quinones) and at our photon fluxes, the excitation of A is much slower than is intersystem crossing, so $k_1 f(t)$ can be regarded as the rate constant of triplet formation; this will hold for most typical carbonyl substrates under the conditions of usual nanosecond laser-flash photolysis experiments.
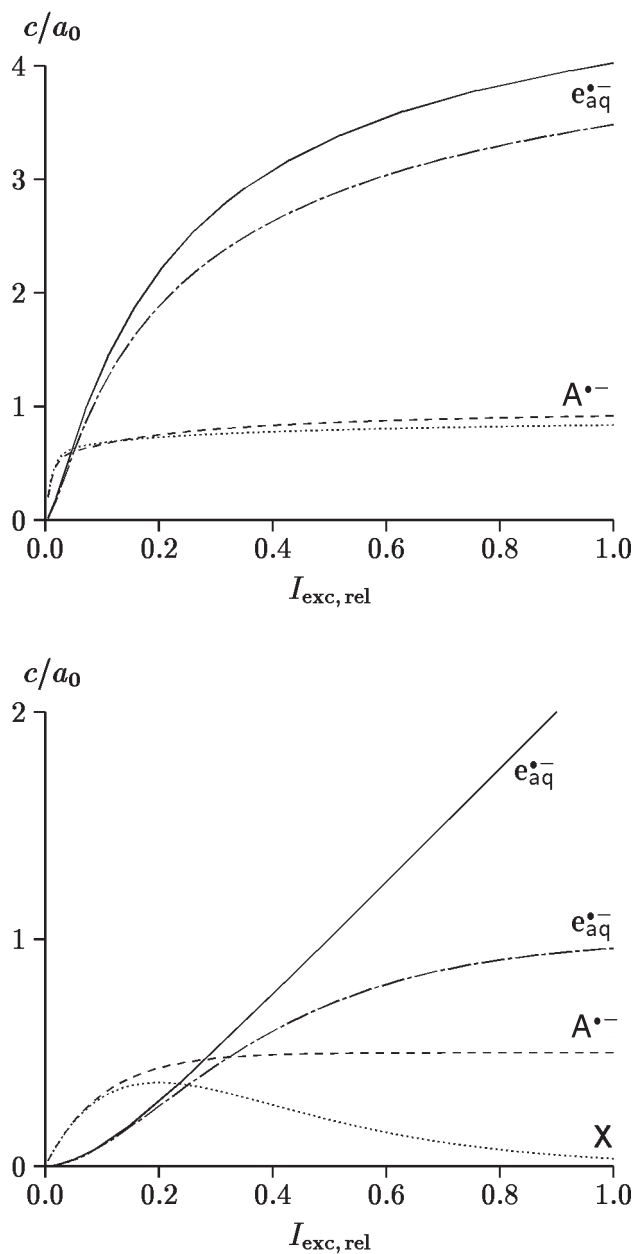
Fig. 1. Simulations based on the kinetic schemes of Schemes 1 and 2 for the concentrations, relative to the substrate concentration a_0, of the intermediates (– – –) and (· · ·) and of the products (—) and (– · – · –) as functions of the relative light intensity, $I_{exc,rel}$. Parameters for all curves: k_d negligible; duration of the laser flash, 20 ns; $k_1 = k_2$. Top trace, cyclic mechanism (Scheme 2), light-dependent steps much faster than quenching ($k_1\overline{f(t)} = 2.5 \times 10^9$ s^{-1}, $k_q = 2.5 \times 10^8$ s^{-1}); (—) and (– – –), rectangular laser pulse; (– · – · –) and (· · ·), triangular laser pulse of the same averaged intensity with identical rise and fall times. Bottom trace, light-dependent steps much slower than quenching ($k_1\overline{f(t)} = 2.5 \times 10^8$ s^{-1}, $k_q = 2.5 \times 10^9$ s^{-1}); (—) and (– – –), cyclic mechanism of Scheme 2; (– · – · –) and (· · ·), sequential mechanism of Scheme 1. The pulse shape has no influence in this case. For further explanation, see text.

Since all other reported two-photon processes with intervening chemical step are irreversible reactions, where excitation of the intermediate **X** does not regenerate the starting material, it is instructive to compare the above results for the cyclic mechanism of Scheme 2 with those for the sequential mechanism of Scheme 1 in this limit of fast quenching. For the latter mechanism, one has [3]

$$[\mathbf{X}]/a_0 = \frac{k_1}{k_2 - k_1} \{ \exp(-k_1 I) - \exp(-k_2 I) \}, \quad (6)$$

$$[\mathbf{e}_{aq}^{\bullet -}]/a_0 = [\mathbf{P}]/a_0 = 1 - \frac{k_2}{k_2 - k_1} \exp(-k_1 I)$$
$$+ \frac{k_1}{k_2 - k_1} \exp(-k_2 I) \quad (7)$$

provided that $k_1 \neq k_2$, or

$$[\mathbf{X}]/a_0 = k_1 I \exp(-k_1 I), \quad (8)$$

$$[\mathbf{e}_{aq}^{\bullet -}]/a_0 = [\mathbf{P}]/a_0 = 1 - (1 + k_1 I) \exp(-k_1 I) \quad (9)$$

in the case $k_1 = k_2$. Although the corresponding expressions for the cyclic and the sequential mechanisms look quite different, their behavior for small I is almost identical. Expansion in I shows that the functions for the intermediates, $[\mathbf{A}^{\bullet -}]$ or $[\mathbf{X}]$, differ only by third and higher order, and those for the products, $[\mathbf{e}_{aq}^{\bullet -}]$ or $[\mathbf{P}]$, are even identical up to and including the third-order terms. This explains why under conditions of low light intensity and conversion, the intensity dependence of the concentration ratio of the product and the intermediate in two-photon cleavage of ketones [12,13] is the same as in two-photon ionization via absorption–electron transfer–absorption [10].

At increasing values of I, the differences between the curves become manifest. As regards the intermediate, a steady state is reached in the cyclic case, $[\mathbf{A}^{\bullet -}]_{\lim} = k_1 (k_1 + k_2)^{-1} a_0$, while in the irreversible reaction this concentration passes through a maximum and then decreases monotonously towards zero. The height of the maximum $[\mathbf{X}]_{\max}$ is $(k_2/k_1)^{k_1/(k_2 - k_1)} a_0$ for $k_1 \neq k_2$; the lower limit of all these maxima occurs in the case of $k_1 = k_2$, where $[\mathbf{X}]_{\max}$ becomes $(1/e)a_0$. Of far greater significance for practical applications is that in the irreversible

case at best all of the starting material can be converted into $\mathbf{e}_{aq}^{\bullet -}$. By contrast, in the cyclic reaction a linear rise in $[\mathbf{e}_{aq}^{\bullet -}]$ is found asymptotically as long as the quenching is sufficiently fast, $[\mathbf{e}_{aq}^{\bullet -}]_{asym} = k_1 k_2 (k_1 + k_2)^{-1} I a_0$. For this catalytic cycle with respect to the starting material **A**, the amount of $\mathbf{e}_{aq}^{\bullet -}$ formed by continuous illumination is thus only limited by depletion of the quencher. Although at first glance Fig. 1 (top), which illustrates the amount of $\mathbf{e}_{aq}^{\bullet -}$ that can be produced *in a given time* seems to suggest the opposite, this characteristic property of the cyclic mechanism remains when quenching becomes rate determining (compare Eq. (A.9) of Appendix A).

3.2. Experimental intensity dependence

Most experiments were carried out with 1,5-anthraquinonedisulfonate as substrate **A**. Water was the solvent throughout, and triethylamine the electron-transfer quencher **D**. Observation was done at 510 and 590 nm, corresponding to an absorption maximum and minimum of the radical anion; $\mathbf{e}_{aq}^{\bullet -}$ possesses a high extinction coefficient at both these wavelengths. The concentrations of $\mathbf{A}^{\bullet -}$ and $\mathbf{e}_{aq}^{\bullet -}$ were extracted from the experimental absorbances A_i at the two wavelengths λ_i with the known [3] extinction coefficients ϵ_i and optical path length d by means of

$$[\mathbf{A}^{\bullet -}] = \frac{A_1 \epsilon_2(\mathbf{e}_{aq}^{\bullet -}) - A_2 \epsilon_1(\mathbf{e}_{aq}^{\bullet -})}{\{\epsilon_1(\mathbf{A}^{\bullet -}) \epsilon_2(\mathbf{e}_{aq}^{\bullet -}) - \epsilon_2(\mathbf{A}^{\bullet -}) \epsilon_1(\mathbf{e}_{aq}^{\bullet -})\} d}, \quad (10)$$

$$[\mathbf{e}_{aq}^{\bullet -}] = \frac{A_2 \epsilon_1(\mathbf{A}^{\bullet -}) - A_1 \epsilon_2(\mathbf{A}^{\bullet -})}{\{\epsilon_1(\mathbf{A}^{\bullet -}) \epsilon_2(\mathbf{e}_{aq}^{\bullet -}) - \epsilon_2(\mathbf{A}^{\bullet -}) \epsilon_1(\mathbf{e}_{aq}^{\bullet -})\} d}. \quad (11)$$

Owing to the secondary reactions of the electron (above all, self-termination and reaction with surplus substrate to give the radical anion), the kinetic traces after the flash exhibit a fast decay of

---

[3] Extinction coefficients of transient species were determined relative to the maximum values, which were taken from the literature: Refs. [14–16] for the species derived from 1,5-anthraquinonedisulfonate, 4-carboxybenzophenone, and for $\mathbf{e}_{aq}^{\bullet -}$, respectively.

$[e_{aq}^{\bullet-}]$ and a slower rise of $[A^{\bullet-}]$. However, as long as no significant amounts of the substrate triplet A^* were present, no extrapolations of the kinetic traces were needed to obtain the values at the end of the flash.

Provided that $[D]$ was larger than about 0.08 M in this system, we found curves for $[e_{aq}^{\bullet-}]$ as functions of the light intensity that were of the same shape as in the bottom trace of Fig. 1, i.e. characterized by a linear growth above a threshold. Besides, no A^* could be detected. It is thus evident that under these conditions the limit of fast quenching is reached, implying that the kinetic parameters can be extracted from the data without any information about the envelope of the laser pulse; a knowledge of the integral over the latter suffices.

Although initially all our samples were optically thin, an inner filter effect arises during the flash because the transients produced increase the optical density noticeably. Not only does this result in an apparent modulation of the pulse envelope, but the constants k_1 and k_2 pertaining to a given volume element are also functions of its distance from the entrance window in the direction of the beam. Because the concentrations of all species involved in the reaction scale with the substrate concentration a_0 (compare Eqs. (1) and (2)), higher a_0 leads to an apparently lower value of the pulse energy and, hence, to apparently lower constants k_1 and k_2. Experimentally, this inner filter effect thus manifests itself by a slight decrease with increasing a_0 of the asymptotic slope of $[e_{aq}^{\bullet-}]$ (Eq. (5)) versus light intensity.

This inner filter effect was corrected for in the following manner. As can be derived from the Lambert–Beer law, the amount of light $I_{abs,i}$ absorbed by species i (absorbance of this species alone, E_i) is given by

$$I_{abs,i} = I_0 \frac{E_i}{E}\left(1 - 10^{-E}\right), \tag{12}$$

where E is the total absorbance of the sample and I_0 is the incident intensity. If the samples would contain a single absorbing species only and would remain optically thin during the flash, expansion of the Lambert–Beer law to first order would be sufficiently accurate

$$I_{abs,i} \approx I_0 2.303 E_i. \tag{13}$$

A comparison of these equations shows that the simple linear relationship (13) may be used provided that I_0 is replaced by an effective light intensity I_{eff}, which is obtained by multiplying I_0 with a correction factor,

$$I_{eff} = I_0 \overline{(1 - 10^E)/(2.303E)}. \tag{14}$$

The overbar denotes averaging over the pulse duration. This procedure is exact in the limit of fast quenching because the concentration curves do not depend on the pulse shape. Because the optical density of our samples remains fairly low during the flash, averaging over the optical path was done by referring the absorbed intensity to the total irradiated volume (see below). This approximation should cause a negligible error.

To obtain the correction function of Eq. (14), the raw end-of-pulse data for $[A^{\bullet-}]$ and $[e_{aq}^{\bullet-}]$ were first fitted with Eqs. (4) and (5), respectively; the substrate concentrations followed from the mass balance. With the known extinction coefficients[3] at the excitation wavelength, the total optical density was then obtained as a superposition of two exponentials, a linear, and a constant term, and averaged analytically. This is equivalent to replacing the time average by an average over the intensity dependence, which is again permissible in the limit of fast quenching because Eqs. (4) and (5) depend on the total intensity only. The effect of the correction is a slight shift of all experimental data points to the left by an amount that increases with I_0 and with a_0.

When all concentrations are measured relative to a_0, and when the inner filter effects are eliminated, the curves for $[A^{\bullet-}]$ and $[e_{aq}^{\bullet-}]$ should neither be dependent on the substrate concentration nor should the quencher concentration play any role as long as quenching is significantly faster than the light-induced steps. Fig. 2 impressively shows that these predictions are correct and that the kinetic treatment of the preceding Section 3.1 is valid. In this graph, both substrate and quencher concentration vary by one order of magnitude, yet all curves coincide within experimental error. All data sets included can be reproduced extremely
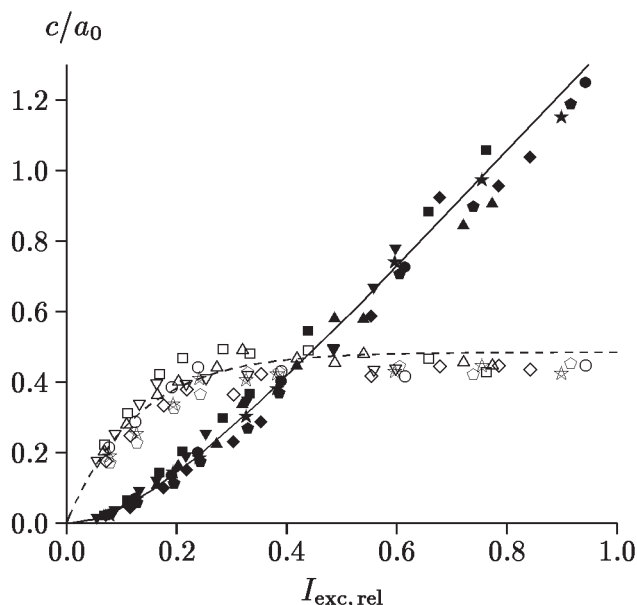
Fig. 2. Photoreaction of 1,5-anthraquinone disulfonate (starting concentration a_0) with the quencher triethylamine in aqueous solution at pH 11. Shown are the concentrations, relative to a_0, of the quinone radical anion (open symbols and dashed fit curve) and of the hydrated electron (filled symbols and solid fit curve) as functions of the relative light intensity, $I_{exc,rel}$. Quinone concentrations in 10^{-5} M, 2.45 (circles), 4.65 (squares), 4.94 (pentagons), 5.12 (stars), 7.78 (diamonds), 10.1 (triangles), and 20.2 (inverted triangles). Quencher concentrations: 0.860 (stars), 0.258 (pentagons), and 0.086 M (all other symbols). Maximum light intensity ($I_{exc,rel} = 1.0$), 36 mJ.

well [4] by one global simultaneous fit of Eqs. (4) and (5) to $[A^{\bullet-}]$ and $[e_{aq}^{\bullet-}]$, which is displayed in the figure. Lastly, the fact that $[e_{aq}^{\bullet-}]$ becomes larger than the substrate concentration is characteristic for the cyclic mechanism of Scheme 2.

The fit curves in Fig. 2 yield $k_1 = 87$ J^{-1} and $k_2 = 94$ J^{-1}. At the highest laser power intensity available, 36 mJ impinge on the sample in 20 ns. This corresponds to rate constants $k_i f(t)$ of about 1.6×10^8 s^{-1} when we assume a rectangular pulse envelope for simplicity. Laser flash photolysis at 355 nm, where photoionization is negligible because $A^{\bullet-}$ does not absorb significantly, and evaluation of the rise of $[A^{\bullet-}]$ gave a quenching

rate constant of 3.9×10^9 M^{-1} s^{-1}. Even at the lowest concentration of **D** in Fig. 2, k_q is thus more than twice as large as $k_1 f(t)$.

When we reduced the quencher concentration further, changes in the shape of $[e_{aq}^{\bullet-}]$ as a function of the pulse energy started to appear, which were consistent with the predictions of Section 3.1. Moreover, the kinetic traces revealed the presence of an increasing amount of A^* at the end of the pulse. A quantitative evaluation proved to be problematic in this case, first because extrapolation of the kinetic traces had to be used to extract the end-of-pulse concentrations of $A^{\bullet-}$ and $e_{aq}^{\bullet-}$, second because the shape of the laser pulse influences the intensity dependence in this limit, and third because the inner filter effect is difficult to correct in this situation. Much more reliable results are expected for $[A^{\bullet-}]$ than for $[e_{aq}^{\bullet-}]$ because the former concentration exhibits the slower post-flash time dependence and the much weaker dependence on the pulse shape (compare Fig. 1). Evaluating the limiting value of $[A^{\bullet-}]$ for high

---

[4] Careful inspection of the plot reveals a slight decrease of $[A^{\bullet-}]$ with increasing light intensity, which might possibly indicate an additional decay channel of photoexcited $A^{\bullet-}$. However, we are inclined to ascribe this to uncertainties of the extinction coefficients of $e_{aq}^{\bullet-}$ at the detection wavelengths. The observed effect can be explained by deviations as small as three percent.

light intensities by using Eq. (A.1) of Appendix A gave a quenching rate constant of 6.5×10^9 $M^{-1} s^{-1}$, in satisfactory agreement with the result from photolysis at 355 nm.

The turnover in each of the two photoinduced steps i of the reaction is obtained by multiplying $I_{abs,i}$ with the pertaining quantum yield ϕ_i ($i = 1, 2$), after converting the pulse energy I_0 into Einsteins and dividing it by the total irradiated volume Ad to average it over the optical path d. The constants k_i finally follow from division by I_0 and by the concentration of the absorbing species. The result is

$$k_i = \frac{2.303 \epsilon_i \phi_i}{A} \frac{\lambda}{hcN_A} \qquad (15)$$

with the respective extinction coefficient ϵ_i, the wavelength λ of the laser, Planck's constant h, the speed of light c, and the Avogadro number N_A.

The extinction coefficients at 308 nm of A and of $A^{\bullet-}$, 2570 and 8000 $M^{-1} cm^{-1}$, were determined by absorption spectroscopy and by laser flash photolysis[3] with UV/VIS detection, respectively. The quantum yields obtained by Eq. (15) from these data and the experimental constants $k_{1,2}$ given above are $\phi_1 = 0.45$ and $\phi_2 = 0.16$. The uncertainties of these values are mostly given by the uncertainties of the extinction coefficients, and are estimated not to exceed 20%. Because quenching of the triplet (lifetime: 140 ns) is almost complete under the conditions used, ϕ_1 can be identified with the intersystem crossing efficiency. A possible reason for the somewhat low value of ϕ_1 is the electronic configuration $(\pi\pi^*)$ of the triplet of 1,5-anthraquinonedisulfonate, as opposed to that of other anthraquinones $(n\pi^*)$ [17]. Determination of ϕ_1 from the limiting yield of radical ions with increasing quencher concentration at very low light intensities or at 355 nm, where photoionization is negligible, gave a consistent value.

In the limit of fast quenching, the ratio of k_1 and k_2 can be extracted directly from the saturation value $[A^{\bullet-}]_{lim}/a_0$ (Eq. (4)), and when the ratio of the extinction coefficients and the quantum yield of radical ion formation are known, the quantum yield of photoionization of $A^{\bullet-}$ can be specified immediately,

$$\phi_2 = \frac{1}{1 + a_0/[A^{\bullet-}]_{lim}} \phi_1 \frac{\epsilon_1}{\epsilon_2}. \qquad (16)$$

This result is not influenced by inner filter effects because these do not affect the saturation concentration. Estimates of k_1 and k_2 in this limit can also be obtained in a very simple way from the point where the curves of $[A^{\bullet-}]$ and $[e_{aq}^{\bullet-}]$ versus laser intensity I_0 cross, provided that this crossing occurs in the region where the former concentration is near the saturation value and the latter has become almost a linear function of I_0 (as in Fig. 2). Denoting the intensity at the point of intersection as I_{int}, we get from Eqs. (4) and (5) by neglecting the exponential terms

$$k_1 \approx \frac{\{2 - [A^{\bullet-}]_{lim}/a_0\}[A^{\bullet-}]_{lim}/a_0}{1 - [A^{\bullet-}]_{lim}/a_0} I_{int}^{-1}, \qquad (17)$$

$$k_2 \approx \{2 - [A^{\bullet-}]_{lim}/a_0\} I_{int}^{-1}. \qquad (18)$$

Both inner filter effects and a remaining curvature work in the same direction, and k_1 and k_2 estimated by Eqs. (17) and (18) constitute upper limits.

These experiments were also performed with 4-carboxybenzophenone, which had previously been investigated by two-flash–two-color laser flash photolysis [11]. Observation was done at 650 nm (absorption maximum of $A^{\bullet-}$) and 800 nm (no absorption of $A^{\bullet-}$); again, $e_{aq}^{\bullet-}$ absorbs strongly at both these wavelengths. The same behavior as that of the quinone was found when the light intensity and the triethylamine concentration were varied. Evaluation in the way described gave $\phi_1 = 0.87$ and $\phi_2 = 0.23$,[5] with comparable uncertainties as in the former system. The value of ϕ_1 in this system is in line with expectation because 4-carboxybenzophenone possesses a quantum yield of intersystem crossing near unity [14]. The higher quantum yield of ionization compared to the radical anion of the quinone is readily

---

[5] The substantially higher value compared to that reported earlier by us [11] for photoionization of the 4-carboxybenzophenone radical anion by 388 nm radiation is ascribed to the fact that at 308 nm a higher excited state of $A^{\bullet-}$ is reached (the absorption spectrum exhibits a minimum at about 320 nm).

explained by the thermodynamically more favorable ionization of the ketone-derived species, the reduction potential of 4-carboxybenzophenone being more negative than that of 1,5-anthraquinonedisulfonate by 0.63 eV [14].

4. Conclusions

The theoretical predictions for the mechanism of two-photon ionization via photoinduced electron transfer shown in Scheme 2 are thus fully corroborated by the experimental results. The characteristic property of this catalytic cycle, namely that the electron yield is not limited by substrate depletion, and the substantial quantum yields induce speculations whether it might also be operative under in vivo conditions, where continuous illumination of small amounts of absorbing electron acceptors (e.g., quinones) in the presence of sacrificial electron donors (e.g., amines or sulfur-containing amino acids [14]) at low intensity levels might nevertheless, in the course of time, produce significant amounts of hydrated electrons. [6]

Appendix A

A solution of Eqs. (1) and (2) can be obtained for a rectangular pulse of duration T and total intensity I, i.e. $f(t) = I/T$ for $t \leqslant T$. To simplify the notation, we set $\kappa_{1,2} = k_{1,2}I/T$. Taking into account the transformation of $\mathbf{A}^*$ into $\mathbf{A}^{\bullet-}$ after the end of the laser pulse, we get for the observed species $\mathbf{A}^{\bullet-}$ and $\mathbf{e}_{aq}^{\bullet-}$:

---

[6] The fast-quenching case (rate-determining photoreactions) with all its implications, especially that the substrate concentration does not limit the amount of $\mathbf{e}_{aq}^{\bullet-}$ that can be formed, is almost ideally realized under these circumstances.

$$[\mathbf{A}^{\bullet-}]/a_0 = \frac{\kappa_1}{\kappa_1(\kappa_2 + k_q) + \kappa_2(k_d + k_q)}$$
$$\times \frac{k_q}{k_d + k_q}\Big\{(\kappa_2 + k_d + k_q)$$
$$- \Big[\kappa_2^2 - \kappa_1(\kappa_2 - k_d + k_q)$$
$$+ (k_d + k_q)^2\Big]\mathscr{S}(\sqrt{w}T)$$
$$- (\kappa_2 + k_d + k_q)\mathscr{C}(\sqrt{w}T)\Big\}, \qquad (A.1)$$

$$[\mathbf{e}_{aq}^{\bullet-}]/a_0 = \frac{\kappa_1\kappa_2 k_q}{\big[\kappa_1(\kappa_2 + k_q) + \kappa_2(k_d + k_q)\big]^2}$$
$$\times \Big\{-(\kappa_1 + \kappa_2 + k_d + k_q) + \big[\kappa_1(\kappa_2 + k_q)$$
$$+ \kappa_2(k_d + k_q)\big]T + \big[\kappa_1^2 + \kappa_2^2$$
$$+ (k_d + k_q)^2 + 2\kappa_1 k_d\big]\mathscr{S}(\sqrt{w}T)$$
$$+ (\kappa_1 + \kappa_2 + k_d + k_q)\mathscr{C}(\sqrt{w}T)\Big\}.$$
$$(A.2)$$

The characteristic root $\sqrt{w}$,

$$w = (\kappa_1 + \kappa_2 - k_d - k_q)^2 - 4\kappa_1(\kappa_2 - k_d) \qquad (A.3)$$

becomes imaginary when the difference $(\kappa_2 - \kappa_1)$ lies within an interval $\pm\sqrt{\kappa_1 k_q}$ around $(k_d + k_q)$. Depending on whether $\sqrt{w}$ is real or imaginary, the functions $\mathscr{S}(\sqrt{w}T)$ and $\mathscr{C}(\sqrt{w}T)$ are given by

$$\mathscr{S}(\sqrt{w}T) = \frac{\sinh(\sqrt{w}T/2)}{\sqrt{w}}$$
$$\times \exp\big[-(\kappa_1 + \kappa_2 + k_d + k_q)T/2\big],$$
$$(A.4)$$

$$\mathscr{C}(\sqrt{w}T) = \cosh(\sqrt{w}T/2)$$
$$\times \exp\big[-(\kappa_1 + \kappa_2 + k_d + k_q)T/2\big]$$
$$(A.5)$$

or

$$\mathscr{S}(\sqrt{w}T) = \frac{\sin(\sqrt{-w}T/2)}{\sqrt{-w}}$$
$$\times \exp\big[-(\kappa_1 + \kappa_2 + k_d + k_q)T/2\big],$$
$$(A.6)$$

$$\mathscr{C}\left(\sqrt{w}T\right) = \cos\left(\sqrt{-w}T/2\right) \\ \times \exp\left[-\left(\kappa_1 + \kappa_2 + k_d + k_q\right)T/2\right]. \tag{A.7}$$

For κ_1 and κ_2 much larger than k_q, $\sqrt{w}$ can be approximated by $(\kappa_1 - \kappa_2)$, and

$$[\mathbf{A}^{\bullet-}]/a_0 \approx \frac{k_q}{k_d + k_q}[1 - \exp(-k_1 I)], \tag{A.8}$$

$$[\mathbf{e}_{aq}^{\bullet-}]/a_0 \approx k_q T\Bigg\{1 - [1/(k_1 I) + 1/(k_2 I)] \\ - \frac{k_2}{k_1(k_1 - k_2)I}\exp(-k_1 I) \\ + \frac{k_1}{k_2(k_1 - k_2)I}\exp(-k_2 I)\Bigg\}. \tag{A.9}$$

Eq. (A.9) shows that in this limit the electron grows asymptotically with $k_q T$, i.e. its formation is limited by the quenching of $\mathbf{A}^*$.

Conversely, when κ_1 and κ_2 are much smaller than k_q, $\sqrt{w}$ can be replaced by $(\kappa_1 + \kappa_2 - k_d - k_q)$. The two smaller rate constants must be retained because the other two cancel in the respective leading term of the functions of Eqs. (A.4) and (A.5). One gets

$$[\mathbf{A}^{\bullet-}]/a_0 \approx \frac{k_1 k_q\left(k_d + k_q\right)^{-1}}{k_1 k_q\left(k_d + k_q\right)^{-1} + k_2} \\ \times \{1 - \exp[-(k_1 + k_2)I]\}, \tag{A.10}$$

$$[\mathbf{e}_{aq}^{\bullet-}]/a_0 \approx \frac{k_1 k_q\left(k_d + k_q\right)^{-1}k_2}{\left[k_1 k_q\left(k_d + k_q\right)^{-1} + k_2\right]^2} \\ \times \Bigg\{-1 + \left[k_1 k_q\left(k_d + k_q\right)^{-1} + k_2\right]I \\ + \exp[-(k_1 + k_2)I]\Bigg\}. \tag{A.11}$$

It is seen that these expressions differ from Eqs. (4) and (5) only by the Stern–Volmer factor $k_q/(k_d + k_q)$ that is associated with k_1 everywhere except in the arguments of the exponentials; for strongly quenched samples ($k_q \gg k_d$), the equations thus become identical.

References

[1] D. Schulte-Frohlinde, M.G. Simic, H. Görner, Photochem. Photobiol. 52 (1990) 1137.

[2] S. Steenken, L. Goldbergerova, J. Am. Chem. Soc. 120 (1998) 3928.

[3] U. Lachish, A. Shafferman, G. Stein, J. Chem. Phys. 64 (1976) 4205.

[4] R.W. Redmont, J.C. Scaiano, L.J. Johnston, J. Am. Chem. Soc. 112 (1990) 398.

[5] J.L. Faria, S. Steenken, J. Phys. Chem. 97 (1993) 1924.

[6] J.L. Faria, S. Steenken, J. Chem. Soc. Perkin Trans. 2 (1997) 1153.

[7] R.A. Holroyd, J. Phys. Chem. 86 (1982) 3541.

[8] P. Natarajan, R.W. Fessenden, J. Phys. Chem. 93 (1989) 6095.

[9] T. Majima, M. Fukui, A. Ishida, S. Takamuku, J. Phys. Chem. 100 (1996) 8913.

[10] V. Zubarev, M. Goez, Angew. Chem. Int. Ed. Engl. 36 (1997) 2664.

[11] M. Goez, V. Zubarev, G. Eckert, J. Am. Chem. Soc. 120 (1998) 5347.

[12] F. Jent, H. Paul, H. Fischer, Chem. Phys. Lett. 146 (1988) 315.

[13] H. Fischer, R. Baer, R. Hany, I. Verhoolen, M. Walbiner, J. Chem. Soc. Perkin Trans. 2 (1990) 787.

[14] I. Loeff, A. Treinin, H. Linschitz, J. Am. Chem. Soc. 115 (1993) 8933.

[15] J.K. Hurley, H. Linschitz, A. Treinin, J. Phys. Chem. 92 (1988) 5151.

[16] J.W.T. Spinks, R.J. Woods, An Introduction to Radiation Chemistry, second ed., Wiley, New York, 1976.

[17] J.M. Moore, D. Phillips, N. Nakashima, K. Yoshihara, J. Chem. Soc. Faraday Trans. 2 83 (1987) 1487.